

Electronic Supporting Information

For *New Journal of Chemistry*

Substituent effect on the N-oxidation of 1,10-phenanthroline derivatives by peroxomonosulfate ion

Ferenc Najóczki, Gábor Bellér*, Mária Szabó, and István Fábián

Department of Inorganic and Analytical Chemistry, University of Debrecen, H-4032 Debrecen,
Egyetem tér 1, Hungary

e-mail: beller.gabor@science.unideb.hu, Tel: + 36 52 512-900/22327, Fax: + 36 52 518-660

TABLE OF CONTENT

Figures

Figure S1A. Representative kinetic curves recorded in the reaction between 4MP and PMS	2
Figure S1B. Representative kinetic curves recorded in the reaction between TMP and PMS	2
Figure S2. APCI-MS identification of HDMPO ⁺	3
Figure S3. APCI-MS identification of HTMPO ⁺	3
Figure S4. APCI-MS identification of H4MPO ⁺	4
Figure S5. APCI-MS identification of H5MPO ⁺	4
Figure S6. APCI-MS identification of H5NPO ⁺	5
Figure S7. APCI-MS identification of H5CPO ⁺	5
Figure S8. Temperature dependencies of the oxidation reactions between the protonated phen derivatives and HSO ₅ ⁻	6
Figure S9. Temperature dependencies of the oxidation reactions between the deprotonated phen derivatives and HSO ₅ ⁻	6

Scheme

Scheme S1. The home-built flow-through titrating system.	7
--	---

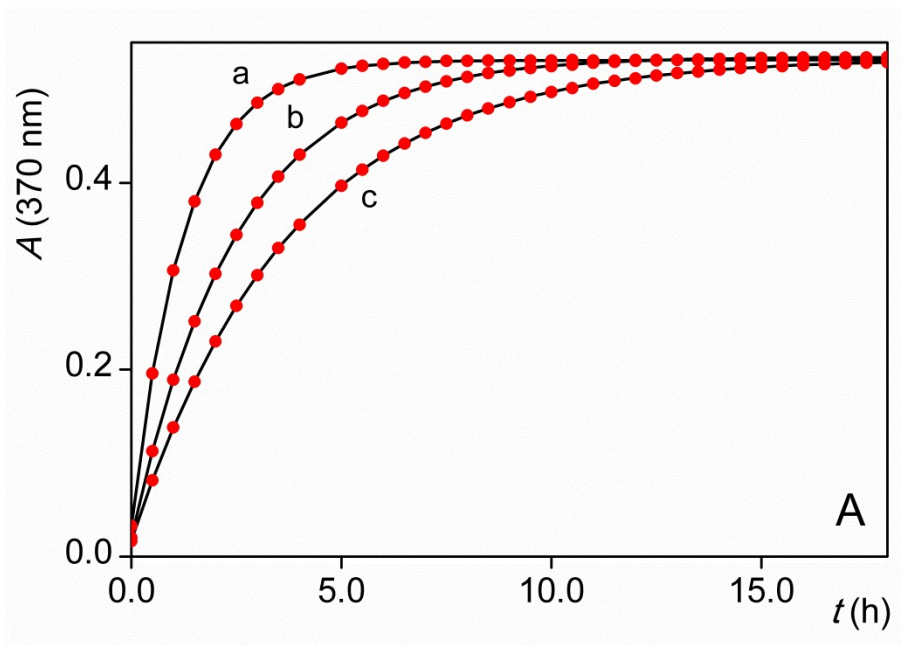


Figure S1A. Representative kinetic traces recorded in the reaction between 4MP and PMS. Circles: experimental data. Only 4% of the recorded points are shown for clarity. Lines: results of the best fit of the data to a single exponential function. $[4MP]_0 = 193 \mu\text{M}$; $[PMS]_0 = 32.4 \text{ mM}$ (a); 16.2 mM (b); 10.8 mM (c); $[H_2SO_4] = 1.00 \text{ M}$; $T = 25.0 \text{ }^\circ\text{C}$; $\lambda = 370 \text{ nm}$; optical path length = 1.000 cm .

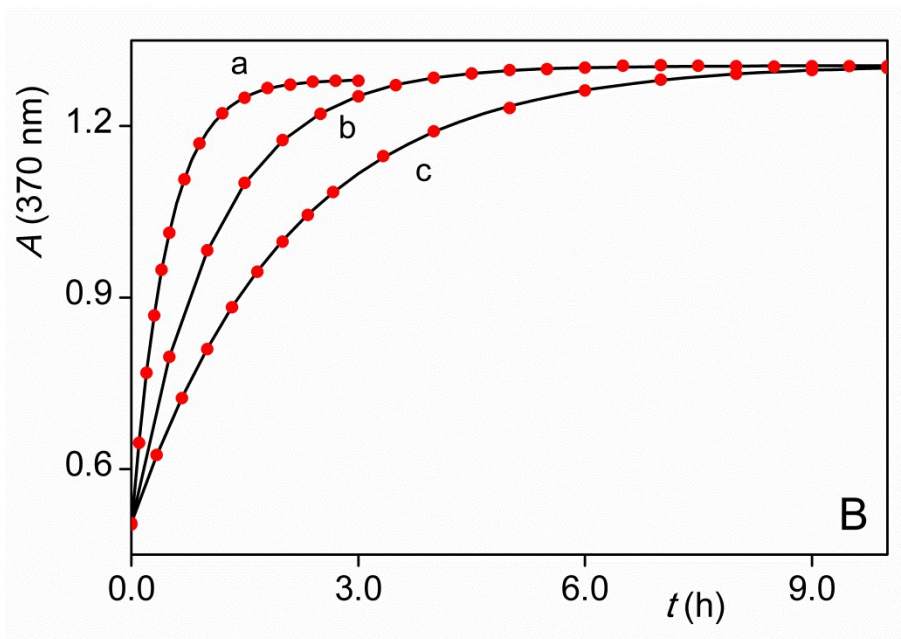


Figure S1B. Representative kinetic traces recorded in the reaction between TMP and PMS. Circles: experimental data. Only 4% of the recorded points are shown for clarity. Lines: results of the best fit of the data to a single exponential function. $[TMP]_0 = 56.6 \mu\text{M}$; $[PMS]_0 = 8.45 \text{ mM}$;

$[\text{H}_2\text{SO}_4] = 1.00 \text{ M}$; $T = 50.0 \text{ }^\circ\text{C}$ (a); $35.0 \text{ }^\circ\text{C}$ (b); $25.0 \text{ }^\circ\text{C}$ (c); $\lambda = 370 \text{ nm}$; optical path length = 1.000 cm .

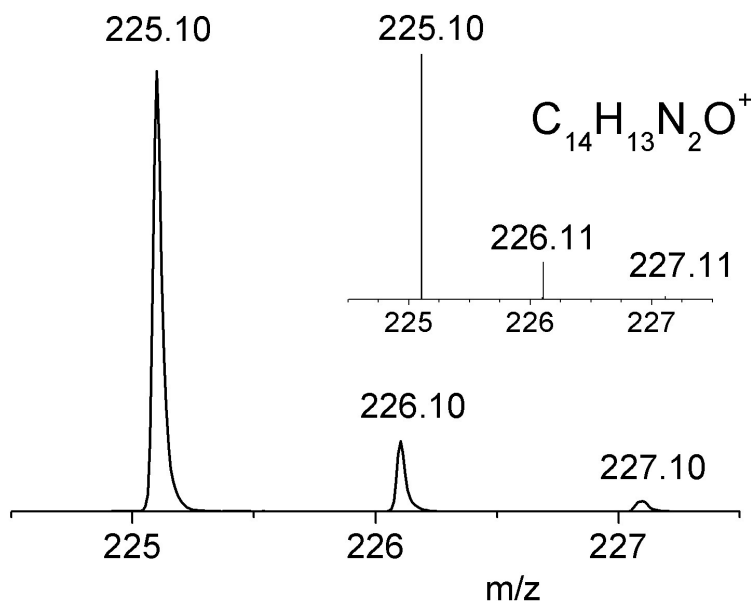


Figure S2. APCI-MS identification of HDMPO⁺ in the reaction mixture of DMP and PMS. $[\text{DMP}]_0 = 0.8 \text{ mM}$; $[\text{PMS}]_0 = 2.6 \text{ mM}$; $\text{pH} \sim 2.5\text{-}3$. Inset: calculated spectrum for the formula C₁₄H₁₃N₂O⁺.

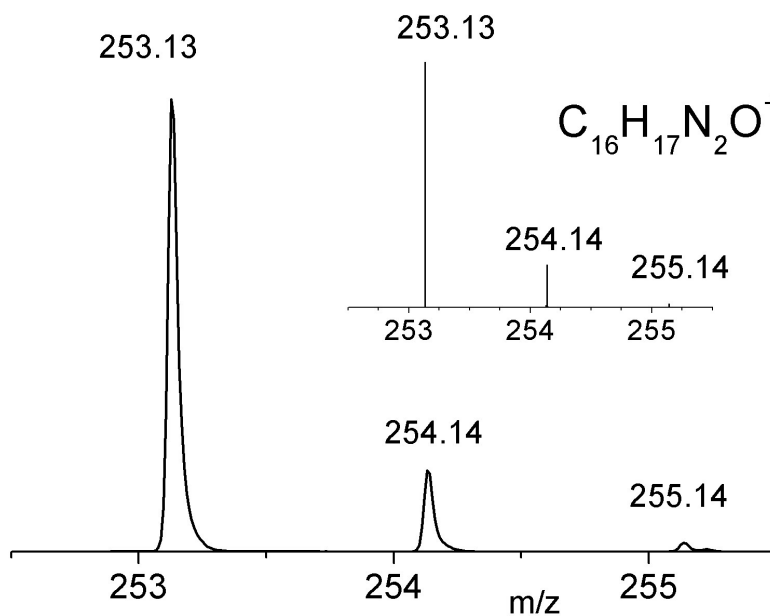


Figure S3. APCI-MS identification of HTMPO⁺ in the reaction mixture of TMP and PMS. $[\text{TMP}]_0 = 0.7 \text{ mM}$; $[\text{PMS}]_0 = 2.5 \text{ mM}$; $\text{pH} \sim 2.5\text{-}3$. Inset: calculated spectrum for the formula C₁₆H₁₇N₂O⁺.

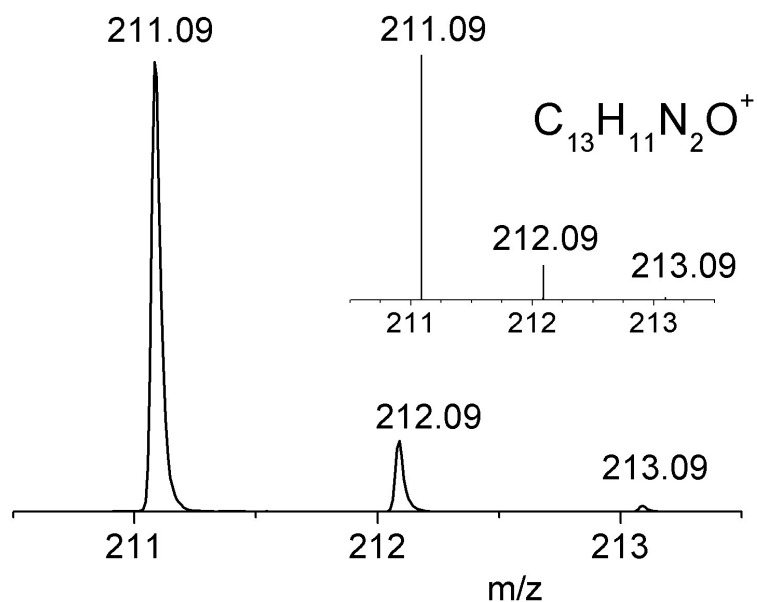


Figure S4. APCI-MS identification of H4MPO⁺ in the reaction mixture of 4MP and PMS. [4MP]₀ = 0.8 mM; [PMS]₀ = 2.5 mM; pH ~ 2.5-3. Inset: calculated spectrum for the formula C₁₃H₁₁N₂O⁺.

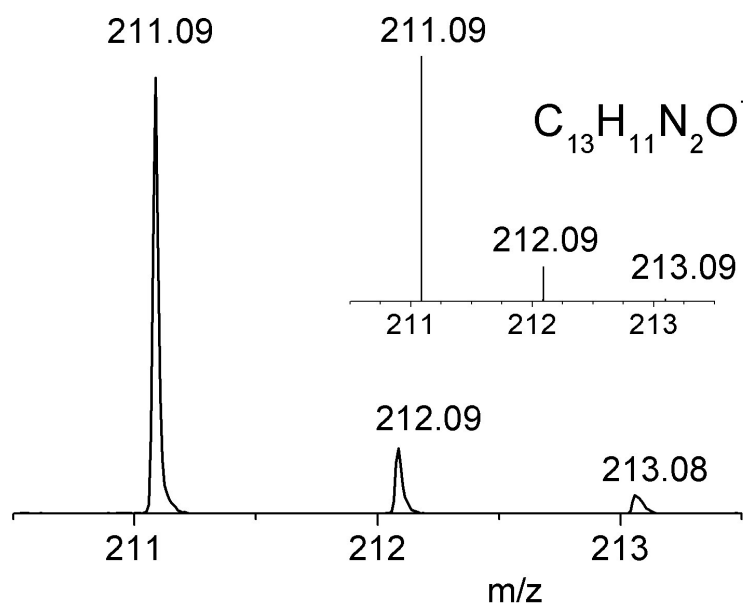


Figure S5. APCI-MS identification of H5MPO⁺ in the reaction mixture of 5MP and PMS. [5MP]₀ = 0.8 mM; [PMS]₀ = 2.7 mM; pH ~ 2.5-3. Inset: calculated spectrum for the formula C₁₃H₁₁N₂O⁺.

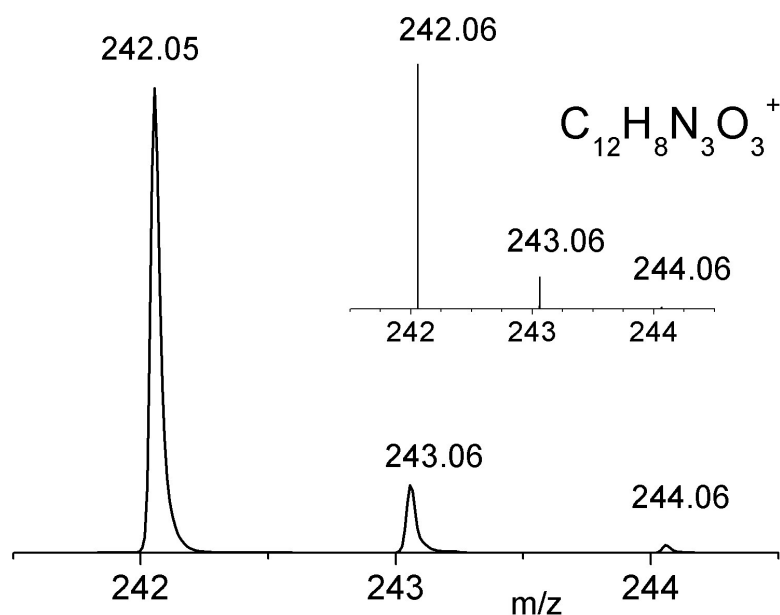


Figure S6. APCI-MS identification of H5NPO⁺ in the reaction mixture of 5NP and PMS. [5NP]₀ = 0.7 mM; [PMS]₀ = 2.6 mM; pH ~ 2.5-3. Inset: calculated spectrum for the formula C₁₂H₈N₃O₃⁺.

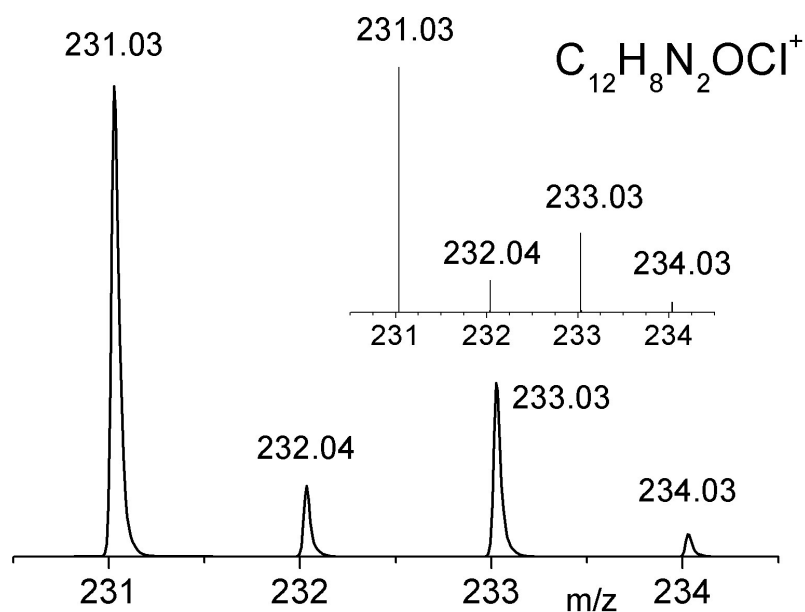


Figure S7. APCI-MS identification of H5CPO⁺ in the reaction mixture of 5CP and PMS. [5CP]₀ = 0.8 mM; [PMS]₀ = 2.5 mM; pH ~ 2.5-3. Inset: calculated spectrum for the formula C₁₂H₈N₂OCl⁺.

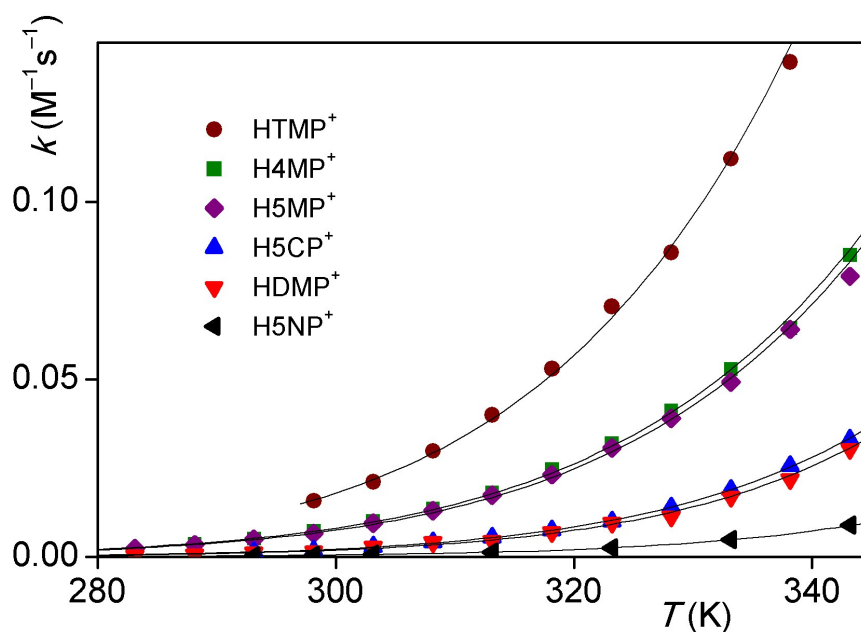


Figure S8. Temperature dependencies of the second-order rate constants of the oxidation pathways of the protonated phen derivatives and HSO_5^- . $[\text{H}_2\text{SO}_4] = 1.00 \text{ M}$, \bullet HTMP $^+$, \blacksquare H4MP $^+$, \blacklozenge H5MP $^+$, \blacktriangle H5CP $^+$, \blacktriangledown HDMP $^+$, \blacktriangleleft H5NP $^+$

Lines: results of the nonlinear fit to the Eyring equation (eq. 12).

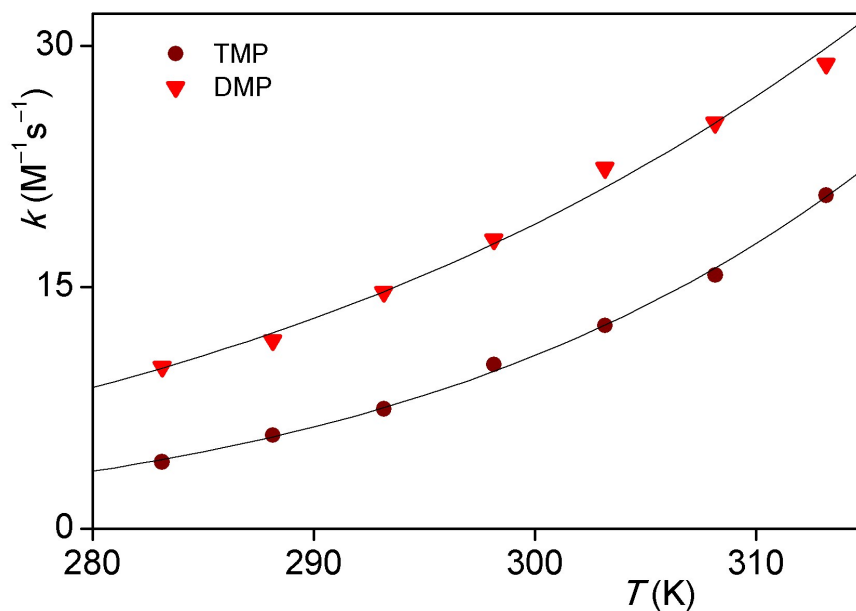
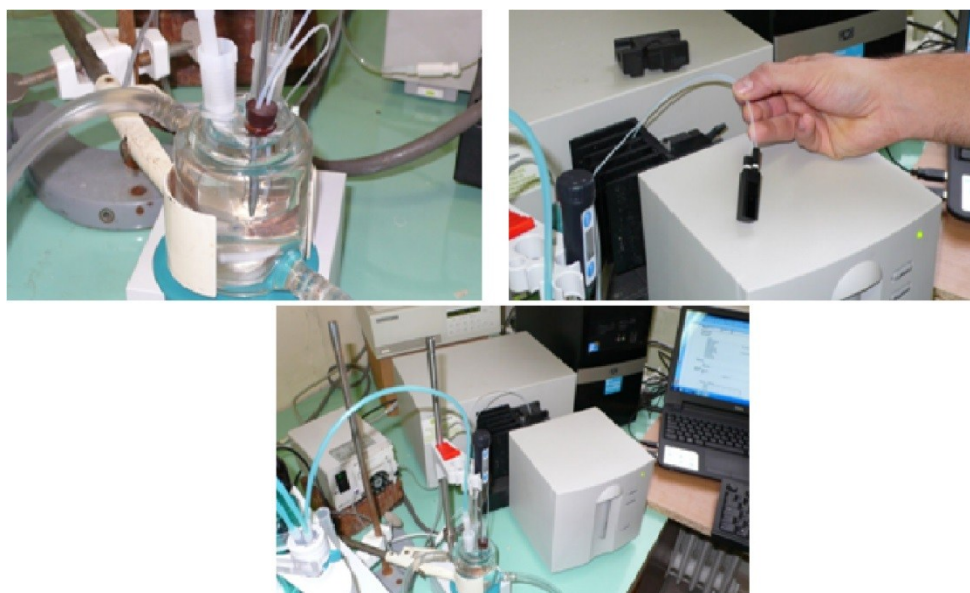


Figure S9. Temperature dependencies of the second-order rate constants of the oxidation pathways of the deprotonated phen derivatives and HSO_5^- . $I = 1.00 \text{ M}$ (NaNO_3), \bullet HTMP $^+$, \blacktriangledown HDMP $^+$

Lines: results of the nonlinear fit to the Eyring equation (eq. 12).



Scheme S1. The home-built flow-through titrating system. Picture 1: The thermostated closed titrating vessel with the pH electrode, the immersed nozzle of the burette and a Pt-100 thermometer. Picture 2: The flow-through optical cell. Picture 3: The complete system.

The pK_{a-s} of DMP, TMP, 5CP, 5NP, and DMPO were determined by a combined pH potentiometric and spectrophotometric method. The spectra of the samples were recorded on a *HP-8453* diode array spectrophotometer at constant temperature in the 200–400 nm wavelength range. Flow-through quartz cuvettes were used with an optical path length of 1.000 cm. Acidified solutions (ionic strength is set to the desired value) were titrated with standardized NaOH solution in a home-built flow-through titrating system.

The central piece of the titrating system is a thermostated closed vessel, which is connected to a flow-through optical cell via a peristaltic pump. The liquid in the vessel is stirred with a magnetic stirrer. The combined pH electrode, a thermometer and the nozzle of the burette are immersed into the vessel. The solution is continuously circulated between the titration vessel and the optical cell, each kept at the same temperature. After adding a sufficient aliquot of titrating solution to the sample, the pH is measured and the spectrum of the solution is recorded with the diode array spectrophotometer equipped with an *HP 89090A Peltier* thermostat. Typically, 50-60 cm³ solution was titrated and the added volume of the titrating NaOH solution

was around 1 cm³ by the end of the titration. Thus, there is a slight change in the ionic strength throughout the titration, but this is negligible for all practical purposes.